



NAGOYA INSTITUTE OF TECHNOLOGY

Nagoya, Japan

June 2012

Design Studies on Less Rare-Earth and High Power Density Flux Switching Motors with Hybrid Excitation/ Wound Field Excitation for HEV Drives

Name	Erwan Bin Sulaiman
Student ID	19517502
Supervisor	Assoc. Prof. Dr. Takashi Kosaka
Department	Graduated School of Engineering, Department of Computer Science and Engineering, Nagoya Institute of Technology
Admission	2009 April
Submitted	2012 June

Abstract

Hybrid electric vehicles (HEVs), using combination of an internal combustion engine (ICE) and one or more electric motors, are widely considered as the most promising clean vehicles. One example of successfully developed electric machines for HEVs is interior permanent magnet synchronous machine (IPMSM), due to its smaller size and lighter weight providing with design freedom of the vehicles and its higher efficiency contributing to less fuel consumption. As an example, from the historical progress of IPMSM installed on Toyota HEVs, the power density of each motor employed in Lexus RX400h'05 and GS450h'06 has been improved five times and more, respectively, compared to that installed on Prius'97. One of the driving forces behind this successful improvement has been the adoption of combination of reduction gear with IPMSM operated at high-speed.

However, IPMSM design tends to be difficult because permanent magnet (PM) is embedded in the rotor core. The mechanical strength relies mainly on thickness and number of bridges around PM, but high number of bridges degrades the maximum torque capability due to increases in leakage flux. Therefore, a new candidate of flux switching machine (FSM) with rugged rotor structure suitable for high-speed operation and the ability to keep high torque and power density is proposed, and examined in this thesis.

This thesis deals with the design studies on high power density hybrid excitation (HE) /field excitation (FE) FSM for HEV drives. Firstly, research background, related works including IPMSM used in HEV, issues of IPMSM for further improvements, and research objectives are discussed in Chapter 1. Then, classifications of FSM and the proposed 12S-10P HEFSM selected for HEV applications are explained in Chapter 2. Under similar restriction and specifications of IPMSM used in HEV, performances of the original 12S-10P HEFSM are examined. Since the initial performances are far from the target requirements, design improvements using "deterministic optimization method" to treat several design parameters are conducted using commercial 2D FEA package, JMAG-Studio ver. 10.0, released by JSOL Corporation. The improved design which successfully achieved the target performances as well as enough mechanical strength being possible to operate at maximum speed of 12,400r/min is discussed in Chapter 3.

Another infirmity of this motor is the presence of high pole numbers, so that the required PWM frequency becomes very high. To reduce the supply frequency of inverter,

various combinations of slot-pole HEFSMs such as 6S-4P, 6S-5P, 6S-7P and 6S-8P are designed and analyzed in Chapter 4.

Among various slot-pole combinations of HEFSMs discussed in Chapter 4, the 6S-5P HEFSM has a better efficiency at high speed operating conditions when compared with other designs, thus it is selected for further analysis. In addition, the problem of high torque ripple of more than 50% in 6S-4P and 6S-8P HEFSMs is difficult to solve. However, to realize high torque and power density, the design motor requires high current density which leads to necessity of complex cooling system to reduce the heat. To overcome this issue, a low-torque, low current density, high-speed and high reduction gear 6S-5P HEFSM-2 is proposed. The target torque is reduced to 210Nm with the introduction of reduction gear ratio of 4:1 to get similar torque axle via reduction gear in IPMSM. Since the rotor mechanical strength is strong enough to operate at high speed, the target speed of the motor is increased to 20,000r/min.

Although the 6S-5P HEFSM-2 has successfully achieved the new target performances, the problem of unbalance pulling force is serious and difficult to overcome. Therefore, the final design of 12S-10P HEFSM discussed in Chapter 3 is selected for further analysis. Even though the proposed machine requires high frequency to operate at high speed, it can be overcome by introducing high frequency switching devices. In addition, it also has no pulling force as well as very less torque ripple which is suitable for high speed HEV applications. Further design reconsiderations are made and the final performances which achieved the target requirements are demonstrated.

Recently the enormous annual usage of rare-earth magnet has increased the price of Neodymium (*Nd*), Dysprosium (*Dy*) and Terbium (*Tb*) which are indispensable to provide the rare-earth magnet with high coercivity as the additives. From view point of cost reduction, the final design 12S-10P HEFSM-2 is analyzed for less rare-earth magnet by reducing the volume of PM in stages. The achieved performances are discussed in Chapter 5.

Finally, by removing all PM in the final design HEFSM discussed in Chapter 5, a new structure of 12S-10P FEFSM is introduced. The results of the initial and improve design which met the target performances are analyzed and discussed in Chapter 6. The prototype model of FEFSM is manufactured and some preliminary experimental results show the proposed FEFSM with no PM is viable candidate for HEV drives.

Contents

1	Introduction	
1.1	Research background	1
1.2	Review on electric motors used in HEV	3
1.3	IPMSM used in HEV	5
1.4	Research objectives	6
1.5	Thesis outlines	7
2	Overview of Flux Switching Machines (FSMs)	
2.1	Introduction	11
2.2	Classifications of Flux Switching Machine (FSM)	11
2.3	Permanent Magnet Flux Switching Machine (PMFSM)	12
2.4	Field Excitation Flux Switching Machine (FEFSM)	16
2.5	Hybrid Excitation Flux Switching Machine (HEFSM)	19
2.6	Selected HEFSM topology for HEV applications	24
2.7	Summary	25
3	Design of 12S-10P HEFSM for HEV applications	
3.1	Design restrictions and specifications	26
3.2	Initial results of the proposed HEFSM	28
3.3	Design methodology for improvements	34
3.4	Results and performances of the final design 12S-10P HEFSM	47
3.5	Summary	58
4	Design and comparison of HEFSM with various slot-pole combinations	
4.1	Introduction	59
4.2	Initial design and performances of 6S-4P, 6S-5P, 6S-7P and 6S-8P HEFSMs	61
4.3	Performances of the final design HEFSMs	65
4.4	Summary	73
5	Design of HEFSM with low-torque high-speed less rare-earth magnet	
5.1	Introduction	75
5.2	6S-5P HEFSM-2	76
5.3	12S-10P HEFSM-2	85
5.4	Design of 12S-10P HEFSM-2 with less rare-earth magnet	90

5.5	Performances of the final design 12S-10P HEFSM-2 with 1.0kg and 0.4kg PM...	95
5.6	Summary	102
6	A new structure of FEFSM for HEV applications	
6.1	Initial design of 12S-10P FEFSM	104
6.2	Initial performances and design improvements of FEFSM	106
6.3	Results and performances of FEFSM based on 2D-FEA	113
6.4	Results and performances of the final design 12S-10P FEFSM based on experimental prototype	119
6.5	Summary	124
7	Conclusion	
7.1	Conclusion	125
7.2	Future works.....	125

List of Figures

Fig. 1.1: Cross sections of traction motors (a) DC motor (b) induction motor (c) PM brushless motor (d) switch reluctance motor	2
Fig. 2.1: Classification of flux switching machines (FSMs).....	11
Fig. 2.2: Examples of PMFSMs (a) 12S-10P PMFSM (b) Fault-tolerance PMFSM (c) E-core PMFSM (d) C-core PMFSM	13
Fig. 2.3: Principle operation of PMFSM.....	15
Fig. 2.4: Example of FEFSMs (a) 1-phase 4S-2P FEFSM (b) 1-phase 8S-4P FEFSM (c) 3-phase 24S-10P FEFSM (d) 3-phase 12S-8P segmental rotor FEFSM.....	16
Fig. 2.5: Principle operation of FEFSM (a) $\theta_e=0^\circ$ and (b) $\theta_e=180^\circ$ flux moves from stator to rotor (c) $\theta_e=0^\circ$ and (d) $\theta_e=180^\circ$ flux moves from rotor to stator.....	18
Fig. 2.6: Example of HEFSMs (a) 6S-4P HEFSM (b) 12S-10P Inner FEC HEFSM (c) 12S-10P Outer FEC HEFSM (d) 12S-10P E-core HEFSM.....	20
Fig. 2.7: The operating principle of the proposed HEFSM (a) $\theta_e=0^\circ$ - more excitation.....	23
Fig. 2.8: Original design of 12S-10P HEFSM [69-70].....	24
Fig. 2.9: Flux paths of PM and FEC of 12S-10P HEFSM.....	25
Fig. 3.1: Main machine dimension of the proposed HEFSM for HEV applications.....	26
Fig. 3.2: Flux path of PM and FEC at open circuit condition (a) Flux path due to mmf of PM (b) Flux path due to mmf of PM and maximum J_e of $30\text{A}/\text{mm}^2$	28
Fig. 3.3: Back-emf of various FEC current density condition at 3000r/min.....	29
Fig. 3.4: Cogging torque of the initial design 12S-10P HEFSM.....	29
Fig. 3.5: Instantaneous torque profile at $J_a = 30\text{A}_{\text{rms}}/\text{mm}^2$, $J_e = 30\text{A}/\text{mm}^2$	30
Fig. 3.6: Torque versus J_e at various J_a	30
Fig. 3.7: Flux vector diagram at $J_a = 30\text{A}_{\text{rms}}/\text{mm}^2$	32
Fig. 3.8: Flux vector diagram at $J_a = 10\text{A}_{\text{rms}}/\text{mm}^2$	33
Fig. 3.9: Torque versus motor circumference in the center of air gap	35
Fig. 3.10: Torque comparison between J_a of $30\text{A}_{\text{rms}}/\text{mm}^2$, J_e of $20\text{A}/\text{mm}^2$ and	36
Fig. 3.11: Simplified design of original 12S-10P HEFSM (a) initial design (b) refined design	37
Fig. 3.12: Enlarged stator yoke of (a) initial design (b) refined design.....	38
Fig. 3.13: Design parameter defined as D_1 to D_{10}	39

Fig. 3.14: Torque versus rotor radius, D_1	41
Fig. 3.15: Torque versus rotor pole depth, D_3	41
Fig. 3.16: Torque versus FEC pitch, D_5	42
Fig. 3.17: Torque versus armature coil width, D_7	43
Fig. 3.18: General flow of the design methodology	44
Fig. 3.19: Comparison between initial and final design 12S-10P HEFSM	46
Fig. 3.20: Main machine dimensions of the final design 12S-10P HEFSM	46
Fig. 3.21: Flux path of the final design at open circuit condition (a) flux path due to mmf of PM only (b) flux path due to both mmf of PM and maximum J_e of $30A/mm^2$	47
Fig. 3.22: Back-emf of the original and final design 12S-10P HEFSM.....	48
Fig. 3.23: Cogging torque of the original and final design 12S-10P HEFSM.....	48
Fig. 3.24: Open circuit field distribution of fluxes at four typical mechanical rotor position (a) $\theta_r = 0^\circ/36^\circ$ (b) $\theta_r = 9^\circ$ (c) $\theta_r = 18^\circ$ (d) $\theta_r = 27^\circ$	49
Fig. 3.25: Torque versus J_e at various J_a of the final design.....	50
Fig. 3.26: Power factor versus J_e at various J_a of the final design.....	50
Fig. 3.27: Torque and power factor of original and final design at maximum J_a and J_e	51
Fig. 3.28: Flux vector diagram of FEC current density at J_a of $30A_{rms}/mm^2$... Error! Bookmark not defined.	
Fig. 3.29: Final torque obtained from FEA and calculated from the flux value	53
Fig. 3.30: Principal stress distributions of rotor at 12,400r/min.....	53
Fig. 3.31: Torque versus speed characteristics of the IPMSM and HEFSM.....	54
Fig. 3.32: Power versus speed characteristics of the IPMSM and HEFSM.....	54
Fig. 3.33: Estimated coil end volume of the final design 12S-10P HEFSM.....	56
Fig. 3.34: Motor losses and efficiencies for operating points shown in Fig. 3.31	57
Fig. 3.35: Iron losses and copper losses distribution	57
Fig. 4.1: Initial design of 6 slot stator yoke HEFSM.....	61
Fig. 4.2: Initial design of rotor pole for slot HEFSMs (a) 4 pole (b) 5 pole (c) 7 pole (d) 8 pole	63
Fig. 4.3: Initial design of 6 slot HEFSMs with various number of poles (a) 6S-4P (b) 6S-5P (c) 6S-7P (d) 6S-8P.....	64
Fig. 4.4: Final design of HEFSMs with various numbers of poles	65
Fig. 4.5: Distribution of flux from PM at open circuit condition (a) 6S-4P	67
Fig. 4.6: Back-emf of the final design HEFSM	68

Fig. 4.7: Torque of the final design HEFSM.....	68
Fig. 4.8: Rotor mechanical stress distribution at maximum speed of 12,400r/min.....	69
Fig. 4.9: Torque versus speed characteristics.....	70
Fig. 4.10: Power versus speed characteristics.....	70
Fig. 4.11: Operating point of HEFSMs.....	71
Fig. 5.1: Design conflictions of general machine.....	75
Fig. 5.2: Torque versus J_e characteristics of 6S-5P HEFSM-1 (Chapter 4).....	78
Fig. 5.3: Initial and final design of 6S-5P HEFSM-2 (a) initial (b) final.....	79
Fig. 5.4: Flux lines of the final designed 6S-5P HEFSM-2 (a) flux from PM only (b) flux from both PM and FEC.....	79
Fig. 5.5: Torque versus J_e characteristics at various J_a	80
Fig. 5.6: Power factor versus J_e at different J_a	80
Fig. 5.7: Torque and power versus speed characteristics.....	81
Fig. 5.8: Principal stress distributions of rotor at 20,000r/min (a) initial design: 210MPa.....	82
Fig. 5.9: Representative operating points of the final design 6S-5P HEFSM-2.....	83
Fig. 5.10: Copper loss, iron loss and eddy current loss of 6S-5P HEFSM-2.....	84
Fig. 5.11: Efficiency of 6S-5P HEFSM-2.....	84
Fig. 5.12: Torque and power versus FEC current density, J_e at maximum armature current density, J_a of $20A_{rms}/mm^2$	86
Fig. 5.13: Main machine dimensions of the final design HEFSM-2.....	87
Fig. 5.14: Flux vector diagram of 12S-10P HEFSM-2 at $J_a = 20A_{rms}/mm^2$	88
Fig. 5.15: Torque and power versus FEC current density, J_e at maximum armature current density, J_a of $20A_{rms}/mm^2$	89
Fig. 5.16: Recent fluctuations in CIF prices of rare-earth metals.....	90
Fig. 5.17: General flow of the design methodology.....	92
Fig. 5.18: Main machine dimensions of the final design HEFSM-2 with 0.4kg PM.....	93
Fig. 5.19: Flux vector diagram of 12S-10P HEFSM-2 at maximum J_a and J_e of $20A_{rms}/mm^2$ and $20A/mm^2$ (a) with 1.0kg PM (b) with 0.4kg PM.....	94
Fig. 5.20: Flux path of the final design 12S-10P HEFSM-2 with 1.0kg and 0.4kg PM at open circuit condition (a) and (c) flux path due to mmf of PM only (b) and (d) flux path due to both mmf of PM and maximum J_e of $20A/mm^2$	95
Fig. 5.21: Principal stress distributions of rotor at 20,000r/min.....	96
Fig. 5.22: Torque and power factor versus J_e at various J_a of the final design 12S-10P HEFSM-	

2 with 1.0kg PM (a) torque versus J_e (b) power factor versus J_e	97
Fig. 5.23: Torque and power factor versus J_e at various J_a of the final design 12S-10P HEFSM-2 with 1.0kg PM (a) torque versus J_e (b) power factor versus J_e	98
Fig. 5.24: Torque and power versus speed characteristic of the final design HEFSM-2 with 1.0kg and 0.4kg PM (a) torque characteristic (b) power characteristic.....	99
Fig. 5.25: Detail loss analysis and motor efficiency of 12S-10P HEFSM-2 with 1.0kg PM...	101
Fig. 5.26: Detail loss analysis and motor efficiency of 12S-10P HEFSM-2 with 0.4kg PM...	102
Fig. 6.1: Main machine dimensions of the proposed 12S-10P FEFSM.....	104
Fig. 6.2: The major flux paths caused by mmf of FEC in 12S-10P FEFSM	105
Fig. 6.3: Design parameters of 12S-10P FEFSM.....	108
Fig. 6.4: Torque versus rotor radius D_1 characteristic	108
Fig. 6.5: Torque versus rotor pole depth D_3 for various rotor pole widths D_2	109
Fig. 6.6: Torque versus excitation coil width D_4 for different excitation coil height D_5	110
Fig. 6.7: Torque and power versus number of turns of armature winding N_a	111
Fig. 6.8: Main machine dimensions of the final design 12S-10P FEFSM.....	111
Fig. 6.9: Open circuit field distribution of FEC at typical rotor electrical positions,	113
Fig. 6.10: Induced voltage of various FEC current densities at 3000r/min	114
Fig. 6.11: Maximum torque waveforms of final design FEFSM based on 2D-FEA.....	114
Fig. 6.12: Torque J_e at various J_a of the final design FEFSM	115
Fig. 6.13: Power factor versus J_e at various J_a of the final design FEFSM.....	115
Fig. 6.14: Principal stress distributions of rotor at 20,000r/min.....	116
Fig. 6.15: Torque and power versus speed characteristics of the final design FEFSM.....	117
Fig. 6.16: Estimated coil end length, L_{end} of the final design 12S-10P FEFSM	118
Fig. 6.17: Prototype of 12S-10P FEFSM (a) stator core (b) armature coil and FEC windings	119
Fig. 6.19: Block diagram of motor torque measurement system	121
Fig. 6.18: Sectional view of the prototype of 12S-10P FEFSM.....	121
Fig. 6.20: Experimental bench	122
Fig. 6.21: Measured and calculated induced voltage at 1000r/min	122
Fig. 6.22: Torque versus armature current (A_{rms}) at various FEC current (AT)	123

List of Tables

Table 1.1: Historical progress in power density of main traction motor installed on Toyota Hybrid Electric Vehicles	6
Table 2.1: Advantages and disadvantages of FSM	22
Table 3.1: Design restrictions and specifications of the proposed 12S-10P HEFSM	27
Table 3.2: Initial and final design parameters of 12S-10P HEFSM	45
Table 3.3: Overall performance of the final design HEFSM	58
Table 4.1: The details of combination between number of stator slots, N_s and number of rotor poles, N_r	60
Table 4.2: Performance comparisons of the initial and final design HEFSMs	66
Table 4.3: Estimated weight, power and torque density of final design HEFSM	71
Table 4.4: Loss and efficiency of 6S-4P and 6S-5P HEFSMs	72
Table 4.5: Loss and efficiency of 6S-7P and 6S-8P HEFSMs	73
Table 5.1: Design requirements, restrictions and specifications of 6S-5P HEFSM-2	77
Table 5.2: Initial and final design parameters of 6S-5P HEFSM-2	78
Table 5.3: Overall performances of the final design 6S-5P HEFSM-2	85
Table 5.4: Initial and final design parameters of 12S-10P HEFSM-2	89
Table 5.5: Initial and final design parameters of HEFSM-2	93
Table 5.6: Overall performances of the final design 12S-10P HEFSM-2	103
Table 6.1: Design restrictions and specifications of FEFSM	107
Table 6.2: Initial and final design parameters of 12S-10P FEFSM	112
Table 6.3: Loss and efficiency of the final design FEFSM	118
Table 6.4: Specifications of the prototype FEFSM	120
Table 7.1: Overall performances of the final design FSM	126

1 Introduction

1.1 Research background

For more than 100 years, vehicles equipped with conventional internal combustion engine (ICE) have been used for personal transportation. In recent days, with rapid increasing rates of world population, demands for private vehicles are also increasing day by day. One of the serious problems associated with ever-increasing use of personal vehicles is the emissions. The enhanced green house effect, also known as global warming, is an acute issue that all people have to face. Government agencies and organizations have developed more stringent standards for the fuel efficiency and emissions. The ICE technology being matured over the past 100 years, nevertheless it will continue to improve with the aid of automotive electronic technology and it will mainly rely on alternative evolution towards improvement in the fuel economy and emission reductions significantly. Therefore, in order to obtain a wide-range full-performance high fuel efficiency vehicle with less-emissions, the most feasible solution at present is the hybrid electrical vehicle (HEV) a combination of battery-operated electric machine with ICE [1-4].

Selection of traction motors for hybrid propulsion systems is a very important step that requires special attention. In fact, the automotive industry is still seeking for the most appropriate electric-propulsion system for HEVs and even for EVs. In this case, key features are efficiency, reliability and cost. The process of selecting the appropriate electric-propulsion systems should be carried out at the system level. Mainly, the choice of electric-propulsion systems for HEV depends on three factors: driver's expectation, vehicle design constraints, and energy source. With these considerations, it is understood that the specific motor operating points are difficult to define [5]. Hence, selecting the most appropriate electric-propulsion system for the HEV is always a challenging task. At present, the major types of electric motors under serious consideration for HEVs as well as for EVs are the dc motor, the induction motor (IM), the permanent magnet synchronous motor (PMSM), and the switched reluctance motor (SRM) [6]. The cross sectional views of each of these four motor types are provided in Fig. 1.1. Moreover, based on the exhaustive review on state of the art of electric-propulsion systems, it is observed that investigations on the cage IMs and the PMSMs are highly dominant, whereas those on dc motors are decreasing but SRMs are gaining much interest [7-10]. The major

requirements of HEVs electric propulsion, as mentioned in past literature, are summarized as follows:

- (i) high instant power and high power density
- (ii) high torque at low speed for starting and climbing, as well as high power at high speed for cruising
- (iii) very wide speed range, including constant-torque and constant-power regions
- (iv) fast torque response

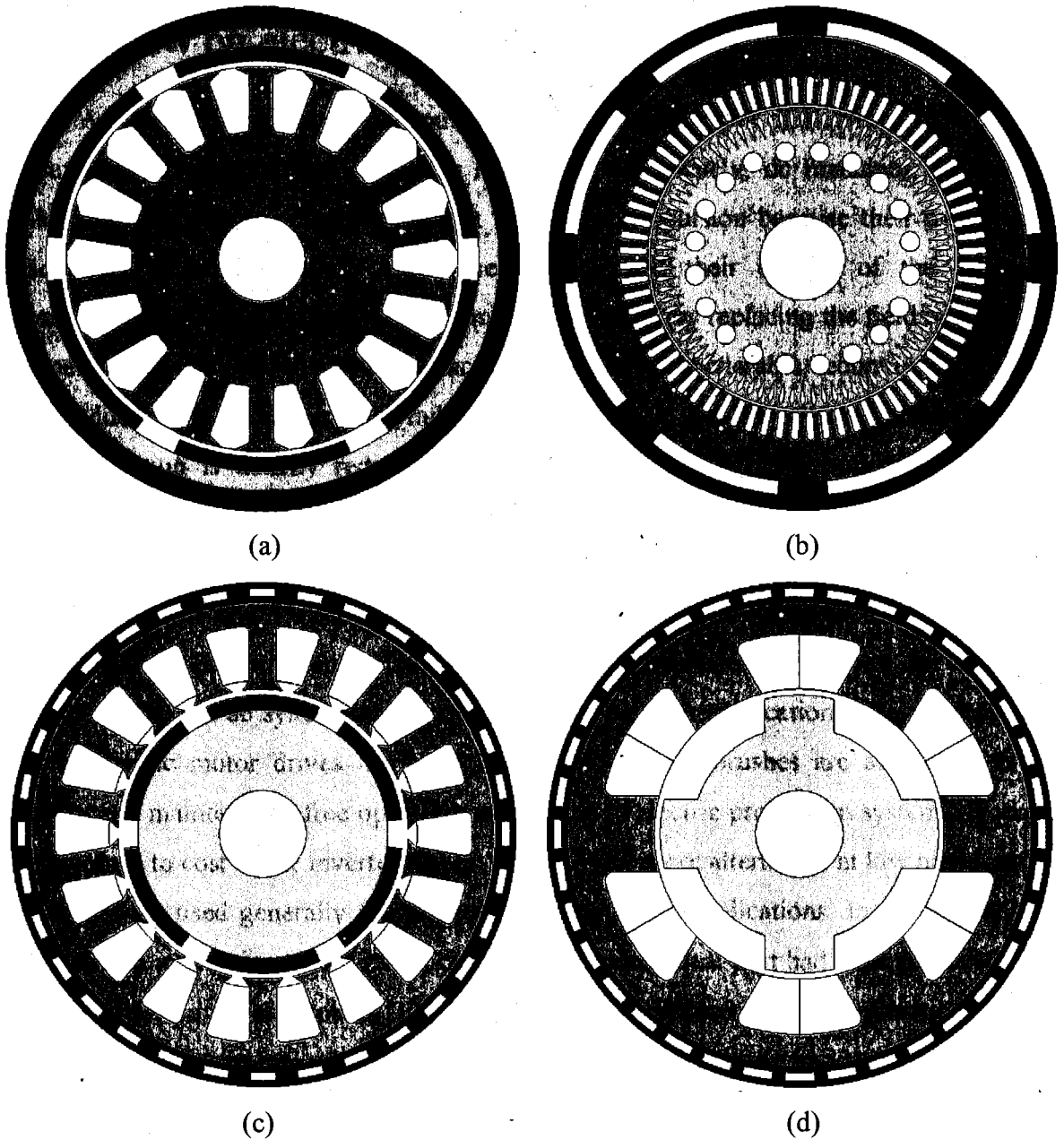


Fig. 1.1: Cross sections of traction motors (a) DC motor (b) induction motor (c) PM brushless motor (d) switch reluctance motor.

- (v) high efficiency over the wide speed and torque ranges
- (vi) high efficiency for regenerative braking
- (vii) high reliability and robustness for various vehicle operating conditions
- (viii) reasonable cost

Furthermore, in the event of a faulty operation, the electric propulsion system should be fault tolerant [11-12]. Finally, an additional selection criterion is the market acceptance degree of each motor type, which is closely associated with the comparative availability of materials and cost of its associated power converter technology [8].

1.2 Review on electric motors used in HEV

As has been mentioned previously, among different types of electric machines, there are four major types that are viable for HEVs and are namely, dc machines, IMs, SRMs, PMSMs. DC motors have been prominent in electric propulsion because their torque-speed characteristics suit the traction requirements well, and their control of the orthogonal disposition of field and armature mmf is simple. Moreover, by replacing the field winding with permanent magnet (PM), the PM dc machines permit a considerable reduction in the stator diameter due to the efficient use of radial space. Owing to the low permeability of PMs, the armature reaction is usually reduced, and the commutation is improved. Since dc motor requires high maintenance mainly due to the presence of the mechanical commutator (brush), as the research advances the brushes are replaced with slippery contacts. Nevertheless, dc motor drives have a few demerits such as bulky construction, low efficiency and low reliability.

With the development of rugged solid-state power semiconductors, the chances to install induction and ac synchronous motor drives in traction applications became feasible by replacing the dc motor drives. In fact, the motors without brushes are attractive, as high reliability and maintenance-free operation add merits to electric propulsion systems. However, with reference to cost of the inverter, the dc motor is still more alternative at low power ratings, as ac drives are used generally for higher power industrial applications. Improvement of the fuel efficiency in existing cars without changing the mechanical part had been achieved by the new dc chopper power electronics [13]. The commutator, if used in proper operation, is a very rugged “inverter”; therefore, the power electronics control circuit can be kept relatively simple and thus at low cost. This is the case of the French automaker PSA Peugeot Citroën, who introduced the HEV version of the well-known Berlingo, which is called Dynavolt, with a dc motor as electric propulsion.

Today, an IM drive is the most mature technology among various brushless motor drives. Cage IMs are widely accepted as the most potential candidate for the electric propulsion of HEVs, due to their reliability, ruggedness, low maintenance, low cost, and ability to operate in hostile environments [7-8]. They are particularly well suited for the rigors of industrial and traction environments. However, the presence of a breakdown torque at the critical speed, limits its extended constant-power operation. Any attempt to operate the motor at the maximum current beyond the critical speed will stall the motor. Moreover, efficiency at a high speed range may suffer in addition to the fact that IMs efficiency is inherently lower than that of PMSM, due to the presence of rotor winding and rotor copper losses [5].

In addition, IM drives have drawbacks such as high loss, low efficiency, low power factor, and low inverter-usage factor, which are more serious for the high speed and large power motor and that pushed them out from the race of HEVs electric propulsion system. Fortunately, these drawbacks are taken into consideration according to the available literatures [14-16].

Meanwhile, SRMs are gaining much interest and are recognized to have a potential for HEV applications. These motors have definite advantages such as simple and rugged construction, low manufacturing cost, fault-tolerant operation, simple control, and outstanding torque-speed characteristics. Furthermore, SRM can inherently operate with an extremely long constant-power range. However, several disadvantages for HEV applications outweigh the advantages. They are acoustic noise generation, torque ripple, necessity of special converter topology, excessive bus current ripple, and electromagnetic-interference (EMI) noise generation. All of the above mentioned advantages and disadvantages are quite critical for vehicle applications. Acceptable solutions to the above disadvantages are needed to get a viable SRM-based HEV [17-18]. Nevertheless, SRM is a solution that is actually envisaged for light and heavy HEV applications [19-20].

On the other hand, PMSMs are becoming more and more attractive and most capable of competing with other motors for the electric propulsion of HEVs. In fact, they are adopted by well-known automakers such as Toyota, Honda, etc., for their HEVs. These motors have many advantages. The overall weight and volume are significantly reduced for a given output power, and it has high power density, high efficiency and high reliability. In addition, the heat generated can be efficiently dissipated to the surroundings. However, due to their limited field weakening capability, these motors are difficult to expand constant power speed region, as the presence of the fixed PM magnetic field.

In order to expand the constant power speed range and improve the efficiency of PMSMs, the power converter can be controlled by six-pulse operation at above the base speed. The speed range may be extended three to four times over the base speed. To realize the wide speed ranges in these motors, an additional dc field excitation coil (FEC) winding is introduced, in such a way that the air-gap field provided by PMs can be weakened during a high-speed constant-power operation by controlling the direction and magnitude of the dc field current which are also called PM hybrid motors. However, at a very high-speed range, the efficiency may drop because of increase in iron loss and also there is a risk of PM demagnetization [7-9].

There are various configurations of the PMSMs which can be classified as surface PMSM (SPMSM) and interior PMSM (IPMSM). The latter is more mechanically rugged due to the embedded PM in the rotor. Although, the SPMSM design uses fewer magnets than the IPMSM, both the motors may achieve a higher air-gap flux density. Another configuration of PMSM is the PM hybrid motor, where the air-gap magnetic field is obtained from the combination of PM and dc FEC as mentioned previously. In the broader term, PM hybrid motor may also include the motor whose configuration utilize the combination of PMSM and SRM. Although the PM hybrid motor offers a wide speed range and a high overall efficiency, the construction of the motor is more complex than PMSM.

In other literatures, the PMSM is also particularly suited for the wheel direct-drive motor applications as in [21]. In addition, a PMSM drives for EV and HEV applications is explained in [22], while the electric motor drive selection issues for HEV applications is also discussed in [23-24].

1.3 IPMSM used in HEV

One example of successfully developed electric machines for HEVs is IPMSM which has been employed mainly to increase the power density of the machines [25-27]. This can be proved by the historical progress in the power density of main traction motor installed on Toyota HEVs as listed in Table 1.1. From the table, the power density of each motor employed in Lexus RX400h'05 and GS450h'06 has been improved approximately five times and more, respectively, compared to that installed on Prius'97 [28]. Although the torque density of each motor has been hardly changed, a reduction gear has enabled to elevate the axle torque necessary for propelling the large vehicles such as RX400h and GS450h. As one of effective strategies for increasing the motor power density, the technological tendency to employ the combination of a high-speed machine and a reduction gear would be accelerated. In spite of

their good performances and well operated, IPMSMs installed in HEV, have some drawbacks to be solved as follows:

- (i) The three-phase armature windings are wound in the form of distributed windings which results in much copper loss and high coil end length.
- (ii) The mechanical stress of the rotor depends on the number of PM bridges. High number of bridges not only increases the mechanically weak points but also causes much flux leakage between the PMs that will degrade the performance of the machine.
- (iii) The present IPMSM has a complex shape and structure which is relatively difficult to perform the design optimization.
- (iv) The constant flux from PM is difficult to control especially at light load high speed operating points.
- (v) The volume of PM used in IPMSM is very high, more than 1.0kg, which increases the cost of the machine.

Table 1.1: Historical progress in power density of main traction motor installed on Toyota Hybrid Electric Vehicles

Model	Year	Max. speed of main traction motor (r/min)	Normalized motor power density (p.u)
Prius	1997	6,000	1.0
Prius	2003	6,700	1.75
RX400h	2005	12,400	4.86
GS450h	2006	14,400	5.61

1.4 Research objectives

In order to avoid such disadvantages, a new machine with concentrated windings which reduces the copper loss and too the coil end length, robust rotor structure for high speed applications, simple shape for ease design optimization, posses an ability to control PM flux, and also operate with less rare-earth magnet such as the flux switching machine (FSM) is identified and selected as the alternative candidate for HEV applications.

The first concept of flux switching machine (FSM) was founded and published in the mid 1950s [29-30]. In [29], a permanent magnet flux switching machine (PMFSM), i.e. permanent magnet (PM) single-phase limited angle actuator or more well-known as Laws

relay, having 4 stator slots and 4 rotor poles was developed, while in [30] it was extended to a single phase generator having 4 stator slots, and 4 or 6 rotor poles. Over the last ten years or so, many novel and new FSM topologies have been developed for various applications, ranging from low cost domestic appliances, automotive, wind power, aerospace, and etc.

Thus, the research objectives of FSMs for HEV applications are listed as follows:

- (i) To design and optimize high power density FSM for HEV applications compared with conventional IPMSM.
- (ii) To design and optimize FSM with less rare-earth magnet for HEV applications
- (iii) To propose and optimize a new structure of FSM without any rare-earth magnet
- (iv) To validate the results experimentally from the prototype of FEFSM

In general FSMs are categorized as PMFSM, hybrid excitation FSM (HEFSM), and field excitation FSM (FEFSM). The classification of FSMs, the operating principle and the proposed hybrid excitation FSM (HEFSM) for HEV applications are discussed in detail in this thesis.

1.5 Thesis outlines

This thesis deals with the design studies on high power density hybrid excitation flux switching machine (HEFSM) and field excitation flux switching machine (FEFSM) for HEV applications. The thesis is divided into 7 chapters and the summary of each chapter are listed as follows:

- (i) Chapter 1: Introduction
The first chapter gives some introduction about the research including research background, related works on HEV and some explanation regarding IPMSM used in HEV. Then problems of current IPMSM used in HEV are highlighted and the research objectives are set to solve the problems.
- (ii) Chapter 2: Overview of Flux Switching Machines (FSMs)
The second chapter explained some introduction and classifications of FSM including the example of PMFSM, HEFSM and FEFSM, the operating principle and the proposed HEFSM for HEV applications.
- (iii) Chapter 3: Design of 12S-10P HEFSM for HEV applications

The third chapter describes the design requirements, restrictions & specifications of the proposed HEFSM with similar restriction and specifications of IPMSM used in HEV. Then, performances of the original 12S-10P HEFSM are examined using commercial 2D-FEA, JMAG-Studio ver. 10.0, released by JSOL Corporation. Since the initial performances are far from the target requirements of 333Nm and 123kW due to flux saturation between armature coil and FEC at high current density condition, design improvements using “deterministic optimization method” to treat several design parameters are conducted until the target performances are achieved. The comparison between the initial and final design 12S-10P HEFSM is discussed. The improved design not only successfully achieved the target performances with much higher power and torque density, but also obtained much higher mechanical strength which is strong enough to operate at maximum speed of 12,400r/min.

(iv) Chapter 4: Design and comparison of various slot-pole combinations of HEFSM

In this chapter, as the other infirmity of the proposed 12S-10P HEFSM in Chapter 3 is the presence of high pole number, the supply frequency becomes more than double of that used in IPMSM. To reduce the supply frequency of inverter, various combinations of slot-pole HEFSMs such as 6S-4P, 6S-5P, 6S-7P and 6S-8P are designed, optimized and analyzed. The design specifications, restrictions and target performances are similar with 12S-10P HEFSM as discussed in Chapter 3. The similar “deterministic optimization method” is used to treat several parameters in effort to achieve the target performances. All final designs with optimum performances are compared and summarized.

(v) Chapter 5: Design of HEFSM-2 with low-torque, high-speed, and less rare-earth magnet

Among various slot-pole combinations of HEFSM discussed in Chapter 4, the 6S-5P HEFSM has a better efficiency, least weight and higher power density compared with the other designs. In addition, the problem of high torque ripple of more than 50% in 6S-4P and 6S-8P HEFSM is difficult to solve. However, to realize high torque and power density, the designed

HEFSM requires high current density which leads to necessity of complex cooling system to reduce the heat. To overcome this issue a low-torque, low current density, high-speed and high reduction gear 6S-5P HEFSM-2 is examined. Hence, the target torque is reduced to 210Nm with the introduction of reduction gear ratio of 4:1 to get similar torque axle via reduction gear in IPMSM. Since the rotor mechanical strength of HEFSM is strong to operate at high speed, the target speed of the motor is elevated up to 20,000r/min. Furthermore, design reconsiderations are made and the final performances which achieved the target requirements are demonstrated. However, although 6S-5P HEFSM-2 has successfully achieved the target performances, the problems of unbalance pulling force are noticed and difficult to overcome. Therefore, the final design of 12S-10P HEFSM in Chapter 3 is selected for further analysis, as the penalty of high frequency inverter can be neglected by introducing high frequency switching devices and also it has no pulling force as well as very less torque ripple. Recently the enormous annual usage of rare-earth magnet has increased the price of Neodymium (*Nd*), Dysprosium (*Dy*) and Terbium (*Tb*) which are indispensable to provide the rare-earth magnet with high coercivity as the additives. From a view point of cost reduction, the final design 12S-10P HEFSM-2 is analyzed for less rare-earth magnet by reducing the volume of PM in stages. The improved and achieved performances of 12S-10P HEFSM with 1.0kg and 0.4kg PM are discussed.

(vi) Chapter 6: A new structure of 12S-10P FEFSM

By removing all PM in the final design 12S-10P HEFSM-2 with 0.4kg PM discussed in Chapter 5, a new structure of 12S-10P field excitation flux switching motor (FEFSM) without PM is introduced. The design specifications, restrictions and target performances are similar with 12S-10P HEFSM-2 mentioned in Chapter 5. The operating principle and the initial design configuration are explained. The results of the initial and improve design which met the target performances are analyzed and discussed. The prototype model of 12S-10P FEFSM is manufactured and some preliminary experimental results are demonstrated for the validation of the proposed machine.

(vii) Chapter 7: Conclusion

The final chapter describes and concludes the summary of the research and pointed out some future works for design improvements. As an example, the overlapped FEC and armature windings in FEFSM should be considered for the design improvement not only to ease the manufacturing process but also to reduce the coil end.

2 Overview of Flux Switching Machines (FSMs)

2.1 Introduction

The first concept of flux switching machine (FSM) was founded and published in the mid 1950s [29-30]. In [29], a permanent magnet flux switching machine (PMFSM), i.e. permanent magnet (PM) single-phase limited angle actuator or more well-known as Laws relay, having 4 stator slots and 4 rotor poles was developed, while in [30] it was extended to a single phase generator having 4 stator slots, and 4 or 6 rotor poles. Over the last ten years or so, many novel and new FSM topologies have been developed for various applications, ranging from low cost domestic appliances, automotive, wind power, aerospace, and etc.

2.2 Classifications of Flux Switching Machine (FSM)

Generally, the FSMs can be categorized into three groups that are permanent magnet flux switching machine (PMFSM), field excitation flux switching machine (FEFSM), and hybrid excitation flux switching machine (HEFSM). Both PMFSM and FEFSM has only PM and field excitation coil (FEC), respectively as their main flux sources, while HEFSM combines both PM and FEC as their main flux sources. Fig. 2.1 illustrates the general classification of FSMs.

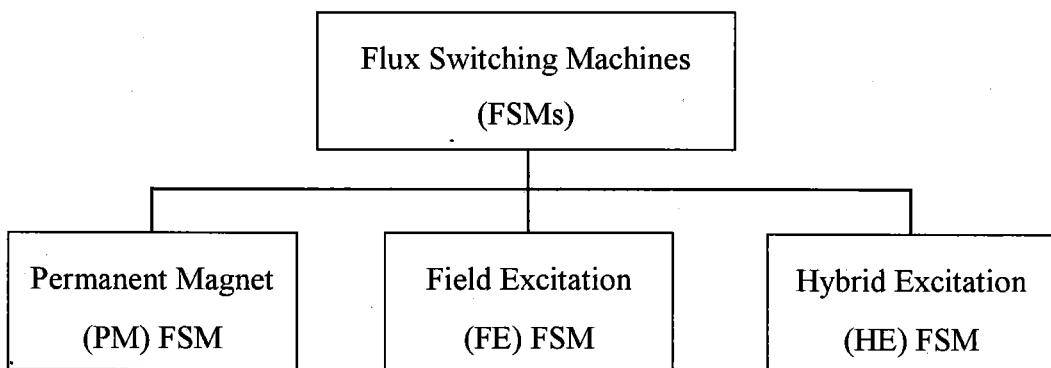


Fig. 2.1: Classification of flux switching machines (FSMs)

2.3 Permanent Magnet Flux Switching Machine (PMFSM)

PM machine based on the principle of flux switching have been studied for several decades. Generally, such machines have a salient pole rotor and the PMs which are housed in the stator. A three-phase FSM based on the homopolar flux principle and the bipolar flux principle have been described in [31–33] and [34–36], respectively, while a new type of single-phase and three-phase PMFSM in which a pair of PMs is embedded on the stator were reported in [37] and [38], respectively. In addition, the performance of Law's relay, a flux-switching type of limited angle actuator was proposed in [39]. Various examples of three-phase PMFSM are illustrated in Fig. 2.2.

Fig. 2.2(a) shows a typical three-phase 12S-10P PMFSM, where the salient pole stator core consists of modular U-shaped laminated segments placed next to each other with circumferentially magnetized PMs placed in between them. For the flux switching principles, the PM magnetization polarity is being reversed from one magnet to another [34-36].

The stator armature winding consists of concentrated coils and each coil being wound around the stator tooth formed by two adjacent laminated segments and a magnet. In the same figure, all armature coil phases such as A1, B1, C1, A2, B2 and C2 have the same winding configuration and are placed in the stator core to form 12 slots of windings. The salient pole rotor is similar to that of SRMs, which is more robust and suitable for high speed applications, and the difference in the number of rotor poles and stator teeth is two. In contrast with conventional IPMSM, the slot area is reduced when the magnets are moved from the rotor to the stator, it is easier to dissipate the heat from the stator and the temperature rise in the magnet can be controlled by proper cooling system.

In addition, since the flux path generated by mmf of the armature windings and PMs are magnetically in parallel, rather than in series as in conventional IPMSM, the influence of the armature reaction field on the working point of the PMs is almost eliminated. As a result, the specific electric loading and the specific torque capability of a PMFSM can be increased. In addition, a high per-unit winding inductance can be readily achieved. Thus, such machines are eminently suitable for constant power operation over a wide speed range, i.e., they can have a high flux-weakening capability [40].

Similar to the fractional-slot PM machine with no-overlapping windings, alternate poles wound windings can also be employed in the three-phase 12S-10P PMFSM in order to be fault-tolerant PMFSM. The armature windings from Fig. 2.2(a) are reduced by removing A2, B2 and C2 to form a total of 6 armature windings as shown in Fig. 2.2(b) [41-42]. In the figure,

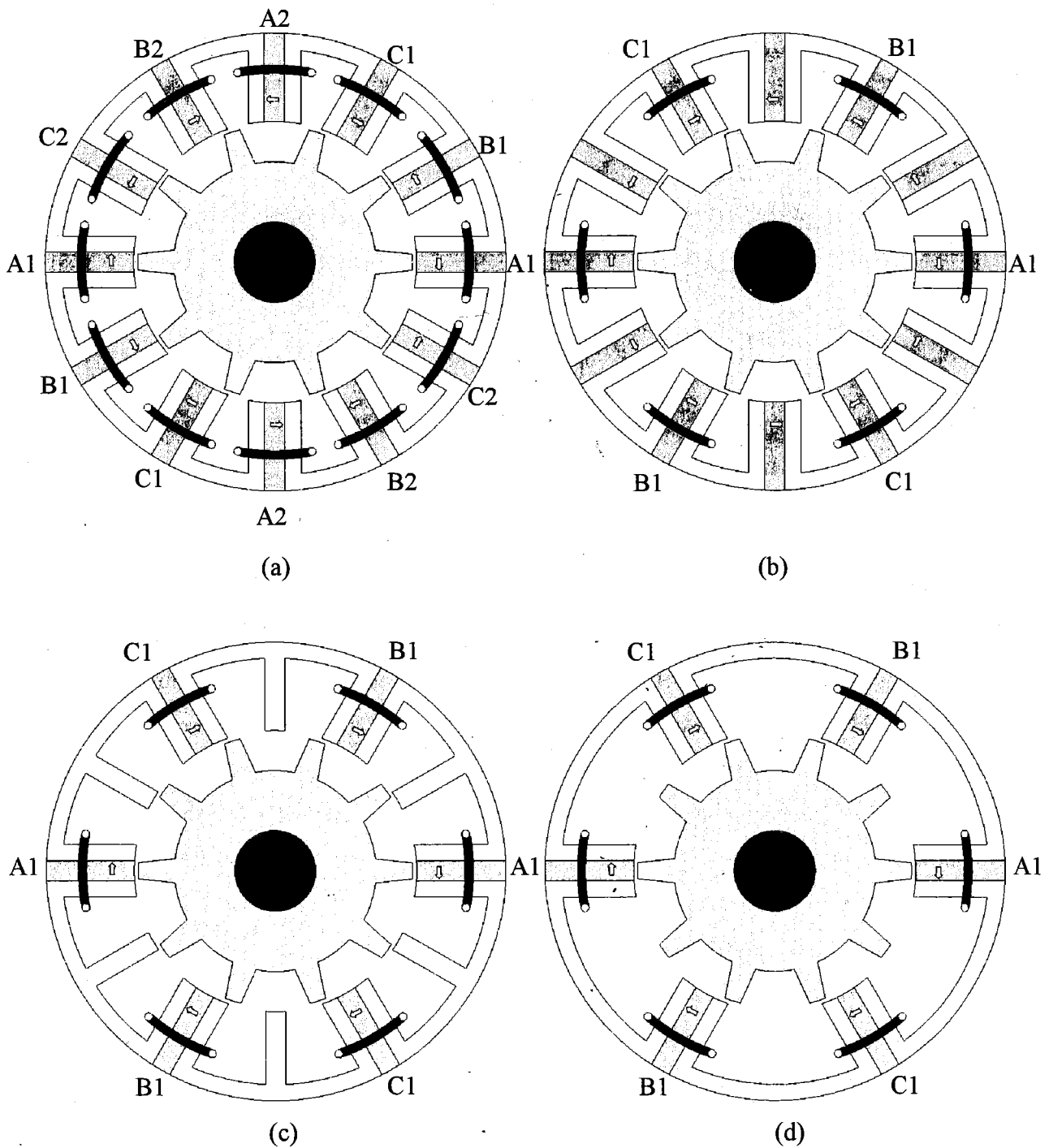


Fig. 2.2: Examples of PMFSMs (a) 12S-10P PMFSM (b) Fault-tolerance PMFSM (c) E-core PMFSM (d) C-core PMFSM

the similar quantity of PM is employed with similar polarity, but with less usage of armature coil which gives the advantages of less copper loss.

However, the conventional PMFSM in Fig. 2.2(a) and (b) have the demerit of high PM volume. Therefore, in order to reduce the usage of PM, the stator poles without armature

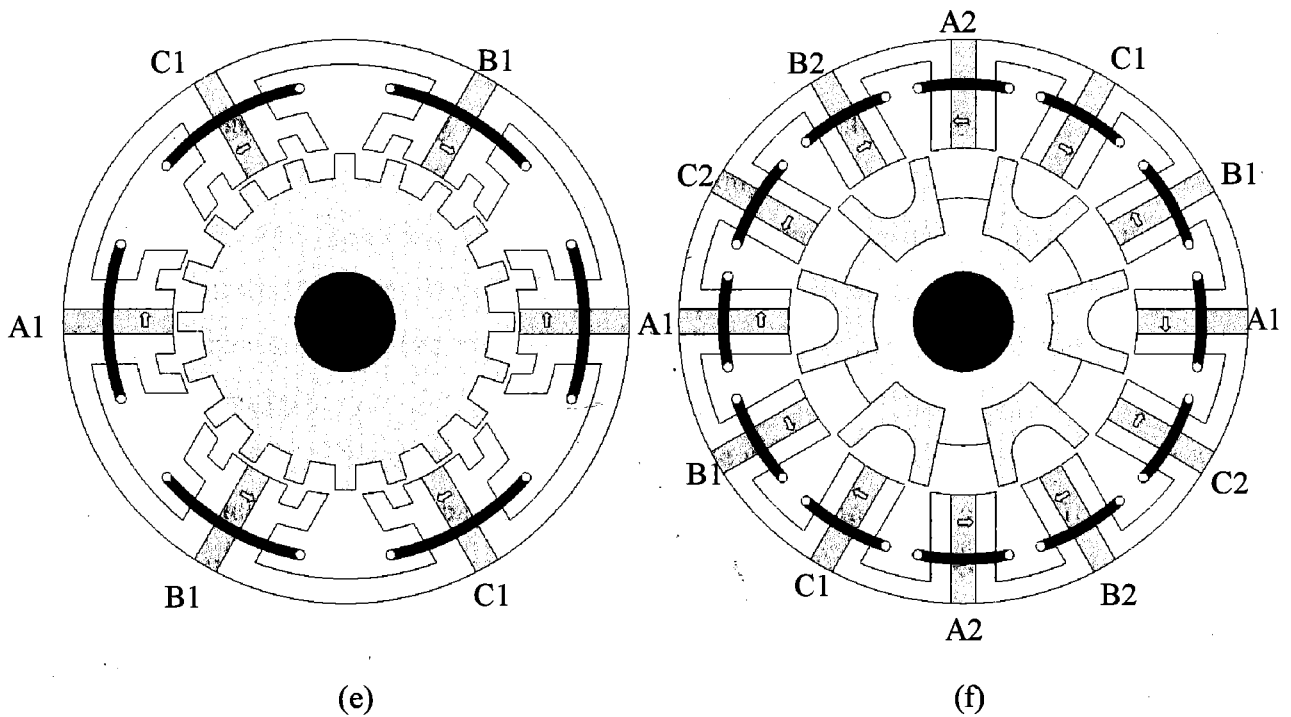


Fig. 2.2: Examples of PMFSMs (e) Multi-tooth PMFSM (f) Segmental rotor PMFSM

winding in the Fig. 2.2(b) are replaced by a simple stator tooth, viz. the new E-core 12S-10P PMFSM is developed as in Fig. 2.2(c) [43-44]. From this figure, half of the PM volume in Fig. 2.2(b) is removed, and the stator core is attached together to form E-Core stator. Further, the middle E-stator teeth can be removed to enlarge the slot area, and consequently the new C-core 6S-10P PMFSM is developed as illustrated in Fig. 2.2(d) [44]. It should be noted that the rotor pole number is close to the stator pole number in the conventional 12S-10P PMFSM, while it is close to twice of the stator pole number in the E- and C-core PMFSM.

In addition, the multi-tooth structure is evolved from the C-core 6S-10P PMFSM to improve the torque density and to reduce the PM usage as shown in Fig. 2.2(e) [45-46]. In the figure, the number of rotor teeth is exactly double when compared with the previous PMFSMs. The end of stator tooth is divided into two parts so that the flux can easily flow to all rotor teeth. However, as the demerits of this multi-tooth PMFSM is high rotor pole numbers, the supply frequency of inverter will also be doubled when compared with the original design.

Finally, a three-phase 12S-10P PMFSM with segmental rotor is also reported as shown in Fig. 2.2(f) [47]. The stator part consists of the similar armature coil and PM as in Fig. 2.2(a), while the rotor is divided into six U shape segments embedded into the shaft steel. The problem of such kind of machine is the rotor mechanical strength which needs to be considered

if the machine is applied for high speed applications. In addition, the summary of various types of PMFSMs are also discussed in [48].

The general operating principle of the PMFSM is illustrated in Fig. 2.3, where the black arrows show the flux line of PM as an example. From the figure, when the relative position of the rotor poles and a particular stator tooth are as in Fig. 2.3(a), the flux-linkage corresponds to one polarity. However, the polarity of the flux-linkage reverses as the relative position of the rotor poles and the stator tooth changes as shown in Fig. 2.3(b), i.e., the flux-linkage switches polarity as the salient pole rotor rotates.

In a few PMFSMs, the flux focusing can be utilized and low-cost ferrite magnets can be implemented. A lumped parameter magnetic circuit model of a 12S-10P PMFSM is established and the design parameters are optimized in [40]. The flux-linkage waveform of a PMFSM is bipolar and the back-emf waveform can be designed to be sinusoidal although concentrated stator winding is employed [49]. The torque production relies on the doubly saliency of both stator and rotor. However, the torque results predominantly from the PM excitation torque whereas the reluctance torque is usually small [35-36]. In the conventional PMFSM, the stator copper area is significantly reduced since both the PMs and armature coils are housed in the stator with high PM volume employed.

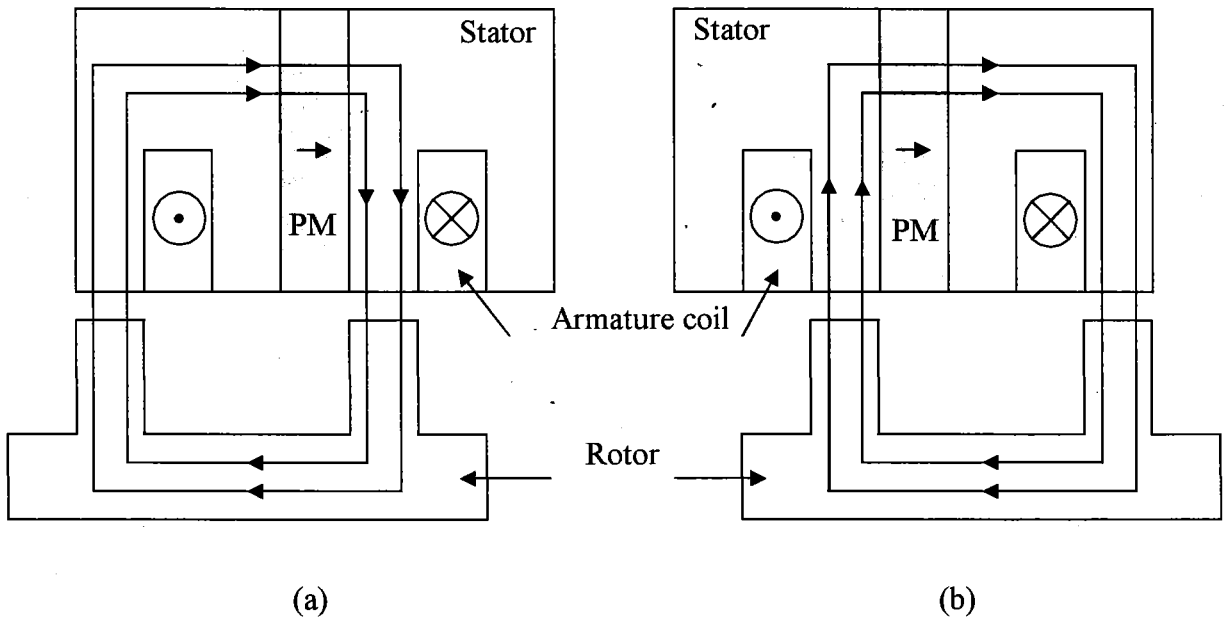


Fig. 2.3: Principle operation of PMFSM

2.4 Field Excitation Flux Switching Machine (FEFSM)

The PM excitation on the stator of conventional PMFSM can be easily replaced by DC FEC to form field excitation flux switching machine (FEFSM) as shown in Fig. 2.4. In other words, the FEFSM is a form of salient-rotor reluctance machine with a novel topology, combining the principles of the inductor generator and the SRMs [50-52]. The concept of the

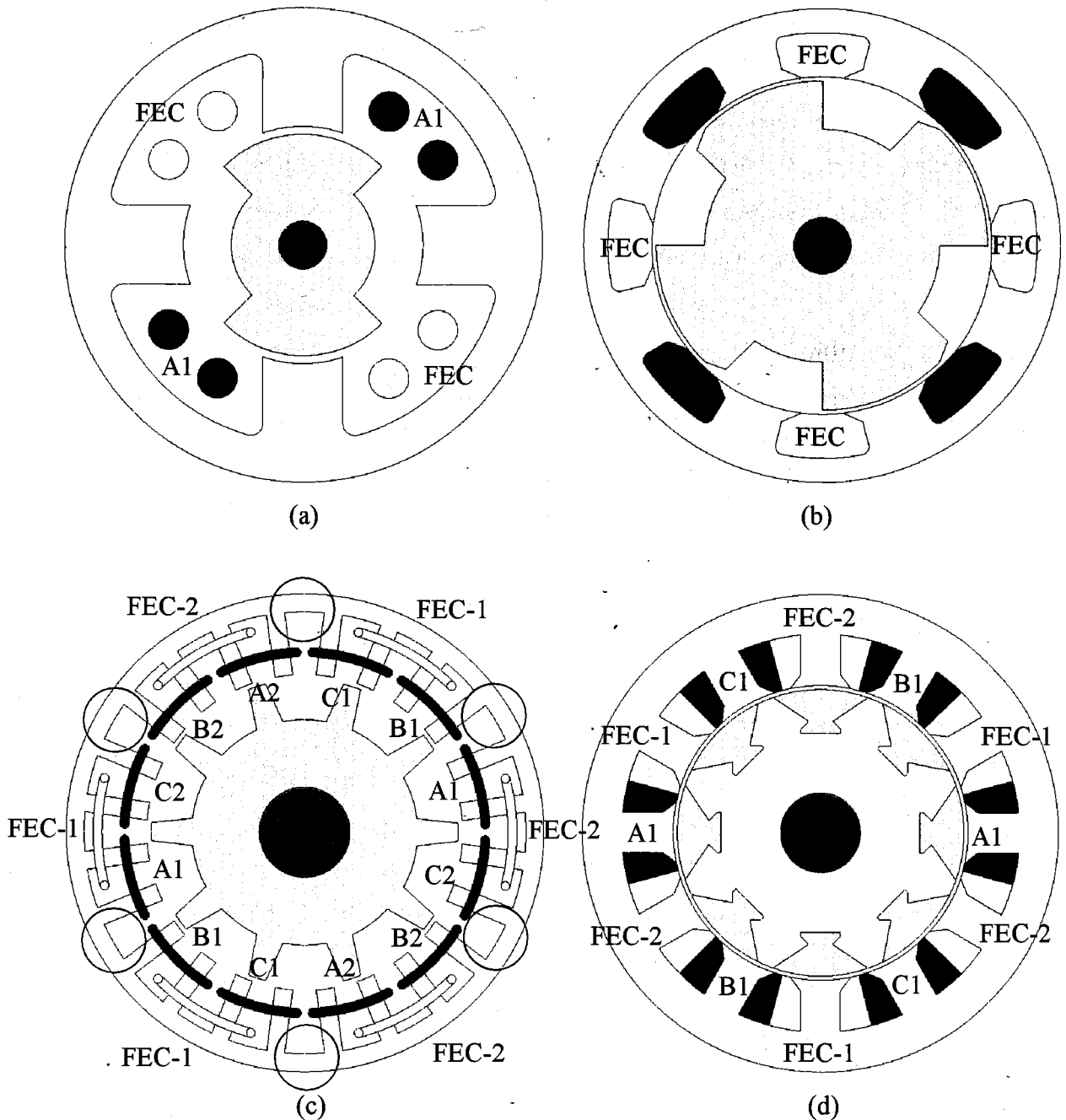


Fig. 2.4: Example of FEFSMs (a) 1-phase 4S-2P FEFSM (b) 1-phase 8S-4P FEFSM (c) 3-phase 24S-10P FEFSM (d) 3-phase 12S-8P segmental rotor FEFSM

FEFSM involves changing the polarity of the flux linking with the armature winding, with respect to the rotor position. Early examples of single-phase 4S-2P FEFSM that employs with a DC FEC on the stator, a toothed-rotor structure and fully-pitched windings on the stator is shown in Fig. 2.4(a) [53]. From the figure, it is clear that two armature coil and FEC windings are placed in the stator which overlapped each other. The viability of this design was demonstrated in applications requiring high power densities and a good level of durability [54–56]. The novelty of the invention was that the single-phase ac configuration could be realized in the armature windings by deployment of DC FEC and armature winding, to give the required flux orientation for rotation. The torque is produced by the variable mutual inductance of the windings. The single-phase FEFSM is very simple motor to manufacture, coupled with a power electronic controller and it has the potential to be extremely low cost in high volume applications. Furthermore, being an electronically commutated brushless motor, it inherently offers longer life and very flexible and precise control of torque, speed, and position at no additional cost.

Another example of single-phase FEFSM is shown in Fig. 2.4(b) with eight stator slots and four rotor poles, 8S-4P FEFSM [57]. From the figure, the FEC winding in four of the slots is fed with direct current to establish four pole magnetic fields. The other four slots contain an armature winding also pitched over two stator teeth. The direction of the current in the armature winding determines, so that a set of four stator poles carries flux and also the position of the rotor. Since the FEC is excited by unipolar current, it can be directly connected in parallel or in series with the dc-supply of power converter which feeds the bipolar current into the armature winding. The design principle is explained in [58], and the single-phase 8S-4P FEFSM has achieved higher output power density than the equivalent induction motor. In addition, the machine also achieved much higher efficiency when compared with the induction machine. However, the single-phase machine has problems of low starting torque, large torque ripple, fixed rotating direction, and overlapped windings between armature coil and FEC.

To improve the performance of the single-phase FEFSM, the three-phase 12S-10P and 12S-8P FEFSMs are developed as shown in Fig. 2.4(c) and (d), respectively. The 12S-10P FEFSM in Fig. 2.4(c) is redesigned from the 12S-10P PMFSM in Fig. 2.2(a) in which the PM is removed from the stator and half of the armature coil slots in the upper layer are placed with the FEC windings as explained in [59]. The FEC-1 and FEC-2 are arranged with alternate DC current source polarity to produce two flux polarities, similar with PM polarity of 12S-10P PMFSM discussed in Fig. 2.2(a). However, since the isolated and unused stator teeth shown in

red circle in Fig. 2.4(c) reduce the performance of the machine, further investigations into improvements of the machine design of three phase FEFSMs should be made.

Finally, the 12S-8P FEFSM is designed with segmental rotor as shown in Fig. 2.4(d) [60-61]. Whereas segmental rotors are used traditionally to control the saliency ratio in synchronous reluctance machines (SynRM), the primary function of the segments in this design is to provide a defined magnetic path for conveying the field flux to adjacent stator armature coils as the rotor rotates. This design gives shorter end windings than the toothed-rotor structure which is associated with overlapping coils. There are significant gains with this arrangement as it uses less conductor materials and also can improve the overall motor efficiency.

The operating principle of the FEFSM is illustrated in Fig. 2.5. Fig. 2.5 (a) and (b) show the direction of the FEC fluxes into the rotor while Fig. 2.5 (c) and (d) illustrate the direction of FEC fluxes into the stator which produces a complete one cycle flux. Similar with PMFSM, the flux linkage of FEC switches its polarity by following the movement of salient

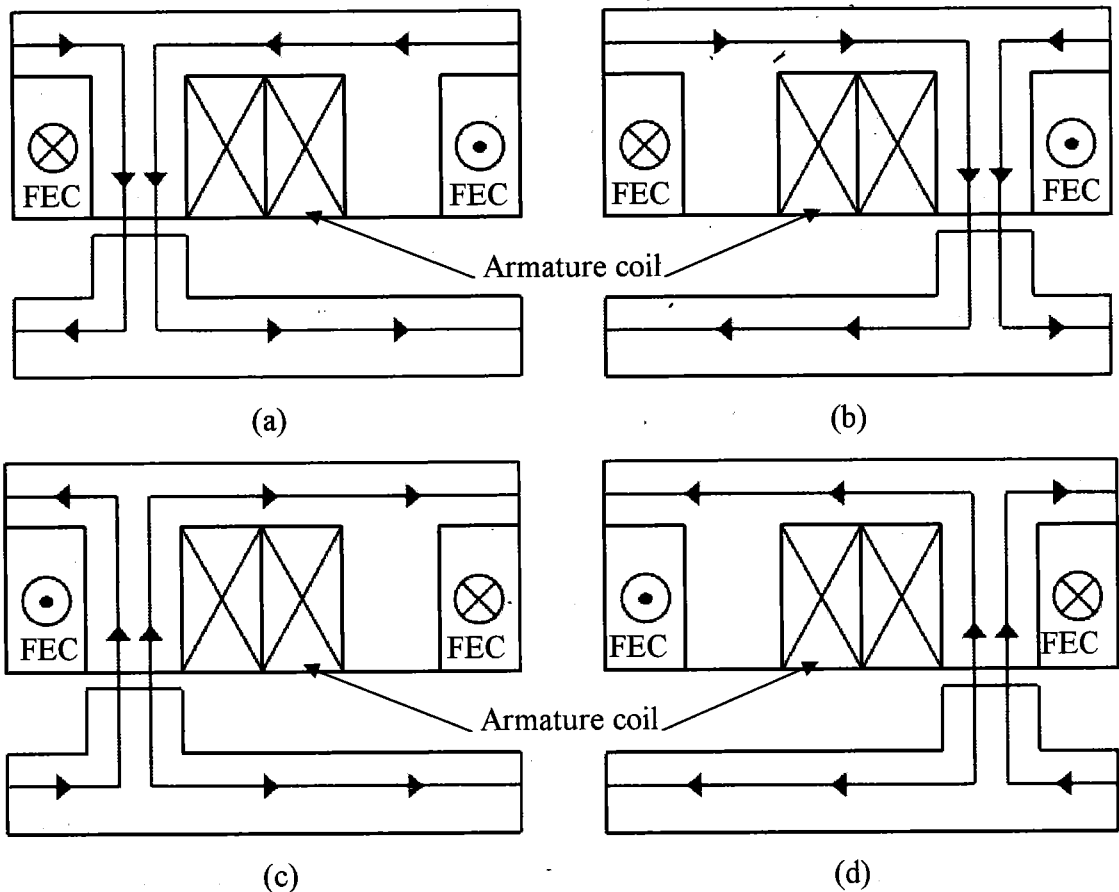


Fig. 2.5: Principle operation of FEFSM (a) $\theta_e=0^\circ$ and (b) $\theta_e=180^\circ$ flux moves from stator to rotor (c) $\theta_e=0^\circ$ and (d) $\theta_e=180^\circ$ flux moves from rotor to stator

pole rotor which creates the term “flux switching”. Each reversal of armature current shown by the transition between Fig. 2.5(a) and (b), causes the stator flux to switch between the alternate stator teeth. The flux does not rotate but shifts clockwise and counterclockwise with each armature-current reversal. With rotor inertia and appropriate timing of the armature current reversal, the reluctance rotor can rotate continuously at a speed controlled by the armature-current frequency. The armature winding requires an alternating current reversing in polarity in synchronism with the rotor position. For automotive applications the cost of the power electronic controller must be as low as possible. This is achieved by placing two armature coils in every slot so that the armature winding comprises a set of closely coupled (bifilar) coils [57]-[62].

2.5 Hybrid Excitation Flux Switching Machine (HEFSM)

Hybrid excitation flux switching machines (HEFSMs) are those which utilize primary excitation by PMs as well as DC FEC as a secondary source. Conventionally, PMFSMs can be operated beyond base speed in the flux weakening region by means of controlling the armature winding current. By applying negative d-axis current, the PM flux can be counteracted but with the disadvantage of increase in copper loss and thereby reducing the efficiency, reduced power capability, and also possible irreversible demagnetization of the PMs. Thus, HEFSM is an alternative option where the advantages of both PM machines and DC FEC synchronous machines are combined. As such HEFSMs have the potential to improve flux weakening performance, power and torque density, variable flux capability, and efficiency which have been researched extensively over many years [63-65].

Various combinations of stator slots and rotor poles for HEFSMs have been developed as illustrated in Fig. 2.6. Fig. 2.6(a) shows a 6S-4P HEFSM in which the active parts are arranged in three layers in the stator. The inner stator consists of the armature windings, followed by the FECs in the middle layer, while the PMs are placed in outer stator as discussed in [66-67]. However, the machine has low torque density and long end winding for the DC FECs, which overlaps the armature windings, and increase copper loss. Moreover, based on the topology of a purely PM excited PMFSM in Fig. 2.2(a), a novel 12S-10P HEFSM is developed [68], in which the PMs dimensions are reduced to save space for the introduced FEC windings, whilst both the stator and rotor laminations are unchanged as depicted in Fig. 2.6(b). It should be emphasized that the flux regulation capability of the machine can be simply controlled by adjusting the PM length in radial direction.

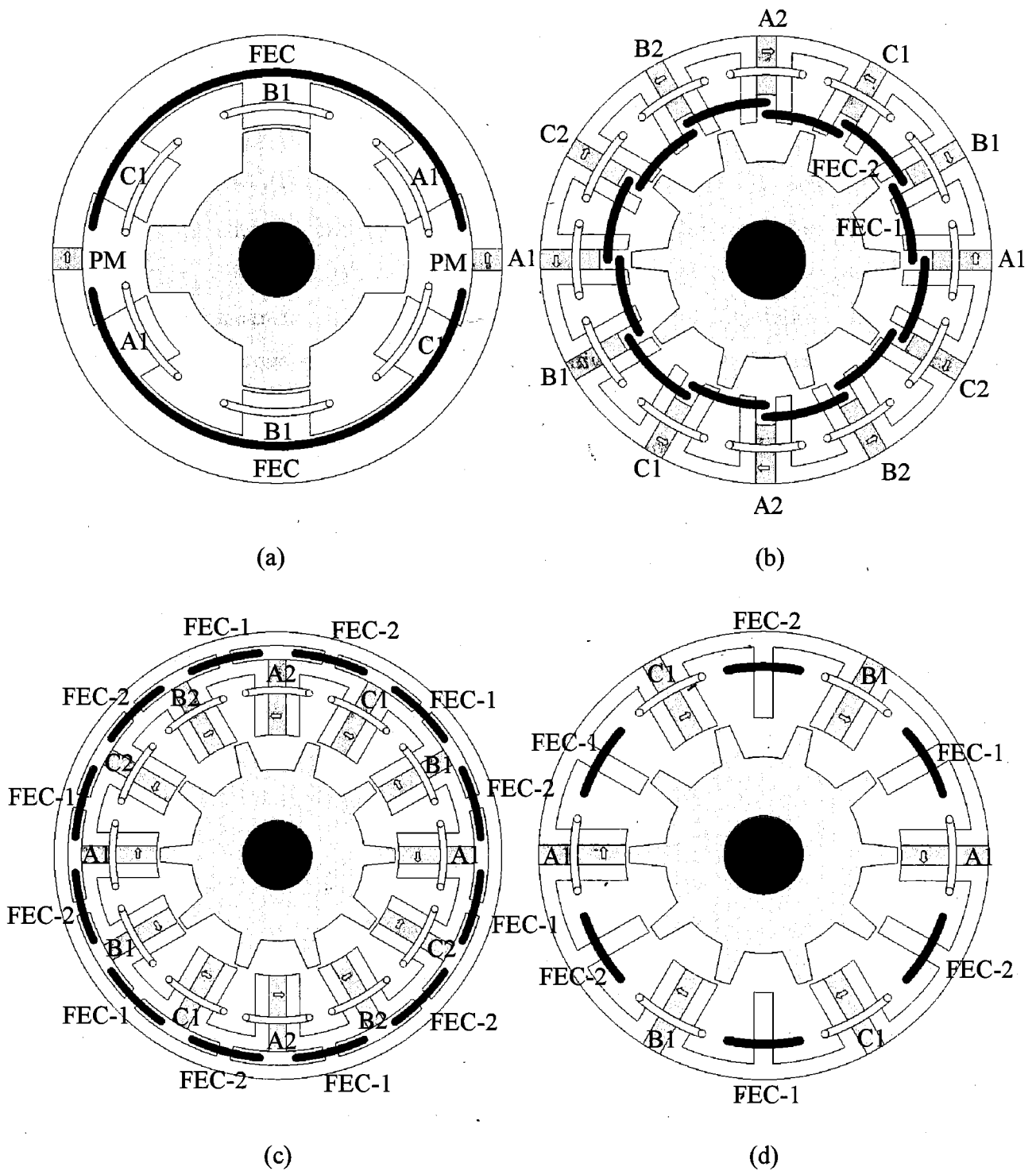


Fig. 2.6: Example of HEFSMs (a) 6S-4P HEFSM (b) 12S-10P Inner FEC HEFSM (c) 12S-10P Outer FEC HEFSM (d) 12S-10P E-core HEFSM

Meanwhile, the HEFSM shown in Fig. 2.6(c) is a 3-phase 12S-10P PMFSM which incorporates the FEC at outer extremity of the stator [69-70]. However, the outer diameter of the machine is significantly enlarged for the FEC winding, which in turn reduces torque density. In addition, the PMs in the PMFSM can be partially replaced by the DC FEC windings

and consequently, several HEFSM topologies were developed as in [71-72]. Although they have no overlapped between the armature coil and FEC, the torque capability is significantly reduced due to less PM volume. The foregoing HEFSMs having magnets on the stator also suffers from one of three disadvantages.

- (i) The DC FEC is in series with the field excited by PMs, which limits the flux-adjusting capability due to low permeability of the PM, Fig. 2.6(a).
- (ii) The flux path of DC FEC significantly reduces the main flux excited by magnets and even short circuits the magnet flux, Fig. 2.6(b) and (c).
- (iii) Torque density may be significantly reduced due to less PM volume, Fig. 2.6(d).

Furthermore, it is clear that to realize the hybrid topology of Fig. 2.6(c), both PM and armature coil volume should be sacrificed, when compared with the conventional 3-phase 12S-10P PMFSM of Fig. 2.2(a), while keeping the machine stator outer radius as constant. From the conventional PMFSM topology, it is possible to replace some of the magnet material with DC FECs and therefore create several HEFSM topologies without loss of armature coil. This represents the simplest method of hybridizing the conventional PMFSM topology with FEC as it retains the existing stator and rotor dimensions and structure.

Furthermore, from the 12S-10P E-core PMFSM mentioned in Fig. 2.2(c) exhibits relatively higher torque density, a new HEFSM is proposed by inserting DC FECs on the middle teeth of the E-core stator, as shown in Fig. 2.6(d) [73]. It maintains the same outer diameter and exhibits a simpler 2-D structure than the HEFSM discussed in Fig. 2.6(c). In addition, it also yields non-overlapping between FEC and armature windings. The number of turns per phase of the E-core HEFSM is maintained same as that of the E-core PMFSM. Half of the slot area is employed for the armature windings, and another half is employed for the dc FECs. The total number of armature winding turns is equal to that of dc FECs to ease the comparison of armature and field currents, because the slot areas for these two kinds of windings are equal. Fig. 2.6(d) also shows the winding connections and the magnetization directions of PMs. It is worth mentioning that, unlike the HEFSM developed from the conventional PMFSM [69-72], the volume of magnet in the E-core HEFSM is maintained as same as in the conventional E-core PMFSM.

However, the HEFSMs in Fig. 2.6(a), (b) and (d) have a PM along the radial of the stator, thus the flux of PM in the outer stator acts as a leakage flux and has no contribution towards the torque production which reduces the machine performance. In addition, due to

segmented stator core, the machine design is also difficult to manufacture. Whereas, the 12S-10P outer FEC HEFSM in Fig. 2.6(c) has no flux leakage outside the stator and it also has the single piece stator which is much easier to manufacture when compared with the other design of HEFSMs. Hence, the machine is considered as the best candidate and is has been selected for further design improvement for HEV applications in this thesis. However, the original 12S-10P outer FEC HEFSM has a limitation of torque and power production in high current density condition due to insufficient stator yoke width between FEC and armature coil slots resulting in magnetic saturation and negative torque production. Thus, the methodology for improvements and the achieved performances are discussed in the following Chapter.

The operating principle of the proposed HEFSM is illustrated in Fig. 2.7, where the red and blue line indicate the flux from PM and FEC, respectively. In Fig. 2.7(a) and (b), since the direction of both PM and FEC fluxes are in the same polarity, both fluxes are combined and move together into the rotor, hence producing more fluxes with a so called hybrid excitation flux. Furthermore in Fig. 2.7(c) and (d), where the FEC is in reverse polarity, only flux of PM flows into the rotor while the flux of FEC moves around the stator outer yoke which results in less flux excitation. As one advantage of the DC FEC, the flux of PM can easily be controlled with variable flux control capabilities as well as under field weakening and or field strengthening excitation. Overview of various FSM, design and performance features, various machine topologies, variable flux capability as well as their relationships with doubly-salient PM machines and flux reversal PM machines are also been discussed in [74]. The advantages and disadvantages of FSM discussed in this chapter are listed in Table 2.1.

Table 2.1: Advantages and disadvantages of FSM

Advantages	Disadvantages
(i) Simple and robust rotor structure suitable for high speed applications	(i) Reduced copper slot area in stator
(ii) Easy to manage magnet temperature rise as all active parts are located in the stator	(ii) Low over-load capability due to heavy saturation
(iii) Flux focusing / low cost ferrite magnets can also be used	(iii) Complicated stator
(iv) Sinusoidal back-emf waveform which is suitable for brushless AC operation	(iv) Flux leakage outside stator
	(v) High magnet volume for PMFSM

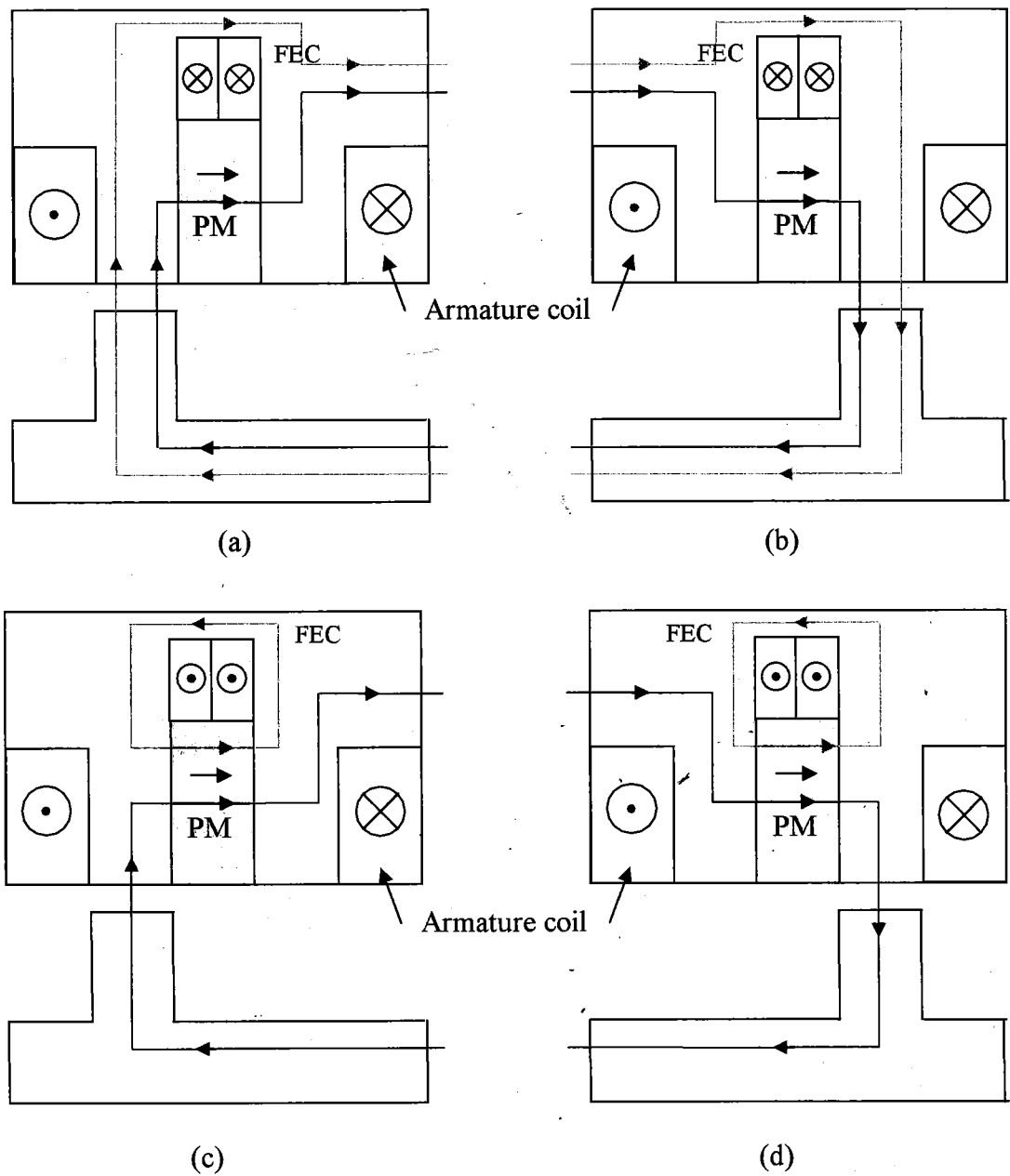


Fig. 2.7: The operating principle of the proposed HEFSM (a) $\theta_e = 0^\circ$ - more excitation (b) $\theta_e = 180^\circ$ - more excitation (c) $\theta_e = 0^\circ$ - less excitation (d) $\theta_e = 180^\circ$ - less excitation.

2.6 Selected HEFSM topology for HEV applications

In this thesis, based on the topology of HEFSM discussed in Fig. 2.6(c), the 12S-10P with outer FEC HEFSM is selected and proposed for HEV applications. Some design studies are conducted in the proposed 12S-10P HEFSM in effort to achieve the target performances of HEV considering design constraints and specifications of IPMSM used in Lexus RX400h [26]. Fig. 2.8 shows the original 12S-10P HEFSM as proposed and discussed in [69-70]. From the figure, it is obvious that the proposed 12S-10P HEFSM is composed of 12 PMs and 12 FECs, distributed uniformly in the midst of each armature coil. The term, “flux switching”, is coined to describe that the stator tooth flux switches its polarity by following the motion of a salient pole rotor. In this machine, the PMs and FECs produce six north poles interspersed between six south poles. The three-phase armature coils are accommodated in the 12 slots. As the rotor rotates, the fluxes generated by the PMs and mmf of the FECs link with the armature coil alternately. For the rotor rotation through $1/10$ of a revolution, the flux linkage of the armature has one electrical periodic cycle and thus, the frequency of back-emf induced in the armature coil becomes ten times of the mechanical rotational frequency.

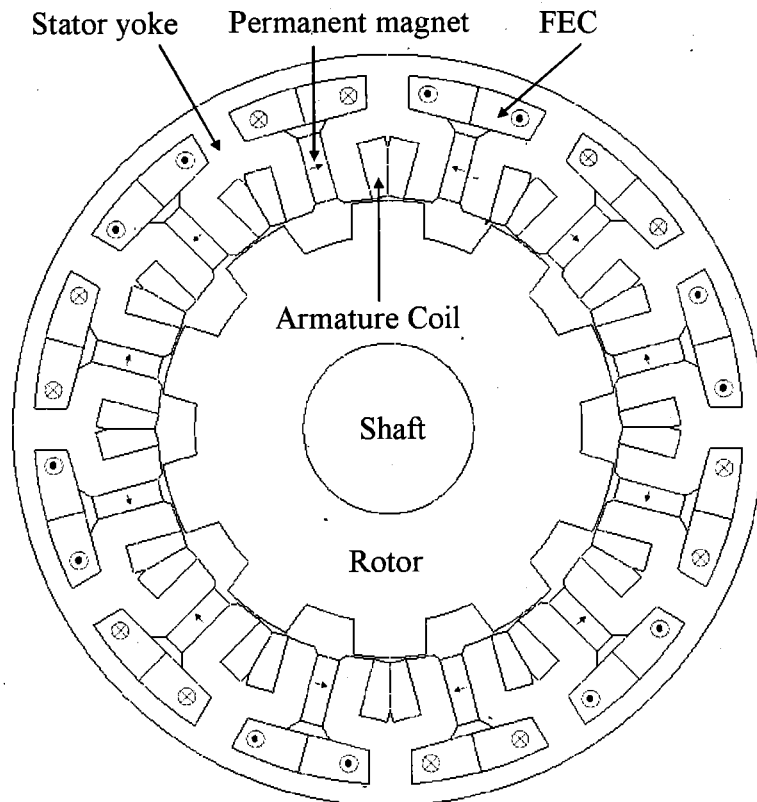


Fig. 2.8: Original design of 12S-10P HEFSM [69-70]

References

- [1] C. Chan: "The state of the art of electric, hybrid, and fuel cell vehicles", Proc. IEEE, Vol. 95, No. 4, pp.704–718, Apr. 2007.
- [2] M. Ehsani, Y. Gao, and J. M. Miller: "Hybrid electric vehicles: architecture and motor drives", Proc. IEEE, Vol. 95, No. 4, pp.719–728, Apr 2007
- [3] D. W. Gao, C. Mi, and A. Emadi: "Modeling and simulation of electric and hybrid vehicles", Proc. IEEE, Vol. 95, No. 4, pp.729–745, Apr 2007
- [4] G. Rizzoni, L. Guzzella, and B. M. Baumann: "Unified modeling of hybrid electric vehicle drivetrains", IEEE Trans. on Mechatronics, Vol. 4, No.3 pp.246–257, Sept. 1999
- [5] Z. Rahman, M. Ehsani, and K. Butler: "An Investigation of Electric Motor Drive Characteristics for EV and HEV Propulsion Systems," SAE Technical Paper, 2000
- [6] L. Eudy, and J. Zuboy: "Overview of advanced technology transportation", National Renewable Energy Lab., U.S, Aug. 2004
- [7] C. C. Chan: "The state of the art of electric and hybrid vehicles," Proc. IEEE, vol. 90, no. 2, pp.247–275, Feb. 2002
- [8] T. M. Jahns, and V. Blasko: "Recent advances in power electronics technology for industrial and traction machine drives," Proc. IEEE, vol. 89, no. 6, pp.963–975, June 2001
- [9] C. C. Chan, and K. T. Chau: "An overview of power electronics in electric vehicles," IEEE Trans. Ind. Electron., vol. 44, no. 1, pp.3–13, Feb. 1997
- [10] K. Rajashekara: "History of electric vehicles in General Motors," IEEE Trans. Ind. Appl., vol. 30, no. 4, pp. 897–904, Aug. 1994
- [11] D. Diallo, M. E. H. Benbouzid, and A. Makouf: "A fault-tolerant control architecture for induction motor drives in automotive applications," IEEE Trans. Veh. Technol., vol. 53, no. 6, pp. 1847–1855, Nov. 2004

- [12] A. G. Jack, B. C. Mecrow, and J. A. Haylock: "A comparative study of permanent magnet and switched reluctance motors for high-performance fault tolerant applications," *IEEE Trans. Ind. Appl.*, vol. 32, no. 4, pp. 889–895, Jul./Aug. 1996
- [13] G. Dancygier et al., "Motor control law and comfort law in the Peugeot and Citroën electric vehicles driven by a dc commutator motor," in *Proc. IEE—Power Electron. and Variable Speed Drives Conf.*, Sep. 21–23, 1998, pp. 370–374
- [14] T. Wang et al., "Design characteristics of the induction motor used for hybrid electric vehicle," *IEEE Trans. Magn.*, vol. 41, no. 1, pp. 505–508, Jan. 2005
- [15] G. Pugslay et al., "New modeling methodology for induction machine efficiency mapping for hybrid vehicles," in *Proc. IEEE Int. Elect. Mach. and Drives Conf.*, Madison, WI, Jun. 1–4, 2003, vol. 2, pp. 776–781
- [16] D. H. Cho et al., "Inductionmotor design for electric vehicle using niching genetic algorithm," *IEEE Trans. Ind. Appl.*, vol. 37, no. 4, pp. 994–999, Jul./Aug. 2001
- [17] J. Malan et al., "Performance of a hybrid electric vehicle using reluctance synchronous machine technology," *IEEE Trans. Ind. Appl.*, vol. 37, no. 5, pp. 1319–1324, Sep./Oct. 2001
- [18] K. M. Rahman et al., "Advantages of switched reluctance motor applications to EV and HEV: Design and control issues," *IEEE Trans. Ind. Appl.*, vol. 36, no. 1, pp. 111–121, Jan./Feb. 2000
- [19] G. Brusaglino, "Energy management optimization by an auxiliary power source," in *dans les Actes du Symp. Véhicules Propres*, La Rochelle, France, Nov. 1993, pp. 223–230
- [20] S. Wang et al., "Implementation of 50-kW four-phase switched reluctance motor drive system for hybrid electric vehicle," *IEEE Trans. Magn.*, vol. 41, no. 1, pp. 501–504, Jan. 2005
- [21] M. Terashima et al., "Novel motors and controllers for high-performance electric vehicle with four in-wheel motors," *IEEE Trans. Ind. Electron.*, vol. 44, no. 1, pp. 28–38, Feb. 1997
- [22] K. T. Chau, C. C. Chan, and Chunhua Liu: "Overview of Permanent-Magnet Brushless Drives for Electric and Hybrid Electric Vehicles", *IEEE Transactions On Industrial Electronics*, Vol. 55, No. 6, June 2008